Supplementary Information

Efficient activation of persulfate by Fe_3O_4@β-cyclodextrin nanocomposite for removal of bisphenol A

Yanyan Zhu[a], Min Yue[b], Natarajan Vinothkumar[a], Lingshuai, Kong[a], Long Ma[c], Yuqiang Zhang[c], Quanqin Zhao[a,*], Jinhua Zhan[a,*]

[a] Key Laboratory for Colloid & Interface Chemistry of Education Ministry, Department of Chemistry, Shandong University, Jinan 250100, P.R. China

[b] School of Environmental Science and Engineering, Shandong University, Jinan 250100, P.R. China

[c] The Testing Center of Shandong Bureau of China Metallurgical Geology Bureau, Jinan, 250100, China

* Corresponding author: E-mail: jhzhan@sdu.edu.cn, zhaoqq@sdu.edu.cn

Tel: +86-0531-8836-5017; Fax: +86-0531-8836-6280

Text S1: Materials

Ferrous sulfate ($FeSO_4 \cdot 7H_2O$), ferric sulfate ($Fe_2(SO_4)_3$), NaOH, potassium persulfate ($K_2S_2O_8$), methanol, ethanol (EtOH) and tert-butyl alcohol (TBA) were provided by Sinopharm Chemical Reagent Co., Ltd (Shanghai, China). BPA, β-CD and 5, 5-dimethyl-1-pyrroline-N-oxide (DMPO) were obtained from Aladdin Chemical Reagent Co., Ltd. Dichloromethane was obtained from Tianjin Fuyu Fine Chemical Co., Ltd (Tianjin, China). All the reagents used were analytical grade and were used as received without further purification. All the solutions were prepared with ultra-pure deionized water. The pH of the solution was adjusted with 0.5 mol/L H_2SO_4 or NaOH.

Text S2: Characterization of the catalysts

The crystalline phase of the catalysts was measured using an X-ray diffractometer (Bruker D8) equipped with a graphite monochromator and Cu Kα radiation (λ = 1.5418 Å) in the range of 10-80°. The morphologies of the catalysts were performed on transmission electron microscope (TEM; JEM-100CXII). Fourier transform infrared (FT-IR) spectra were recorded on a Bruker VERTEX-70 infrared spectrometer in the range of 4000-500 cm^{-1}. And the Brunauer-Emmett-Teller (BET) sorptometer was used to characterize the specific surface area of the catalysts. X-ray photoelectron spectroscopy (XPS) data were recorded on an ESCALAB 250XI spectrometer (Thermo Electron Corporation) in the range of 0-1000 eV to investigate the chemical constitution of the obtained catalyst. The magnetic properties were described with a multi-function vibrating sample magnetometer (VSM; VersaLab) at room temperature. TGA curves of catalysts were recorded on a thermal analyzer (SDT Q600, USA) under nitrogen atmosphere at a heating rate of 10 °C/min.

Text S3: The determination of BPA degradation intermediates with GC−MS

The aromatic degradation intermediates of BPA were determined by GC−MS using an Agilent Technologies (USA) system consisted of a 7890B model GC connected to an Agilent capillary column (HP-5MS, 30 m × 0.25 mm × 0.1 mm), combined with a 5977B model MS. Prior to GC−MS analysis, the oxidation intermediates were extracted with dichloromethane for several times. The solution extracted was dehydrated with anhydrous sodium sulfate and

concentrated to 1 mL by nitrogen gas blowing. The GC oven temperature program was as follows: initial temperature 80 °C for 1 min, followed by heating at 6 °C/min to 300 °C and held at 300 °C for 1 min. Helium was used as the carrier gas at a flow rate of 1.0 mL/min. The mass spectra were recorded with 70 eV electron impact (EI) mode at an ion source temperature of 230 °C. The MS detector was operated in a full scan mode (m/z 50−500) for qualitative analysis. The detected peaks were identified according to the library of Agilent Technologies and NIST data.

Table S1. Summary of physicochemical properties and catalytic activity of different catalysts

Catalyst	Particle size (nm)	S_{BET} ($m^2 g^{-1}$)	Pore volume ($cm^3 g^{-1}$)	M_s (emu g^{-1})	Removal of BPA after 120 min (%)
Fe_3O_4	10-20	71.40	0.4993	73.84	83
Fe_3O_4@β-CD	5-10	104.19	0.5941	66.44	100
reused Fe_3O_4@β-CD	5-10	119.80	0.3930	65.29	86

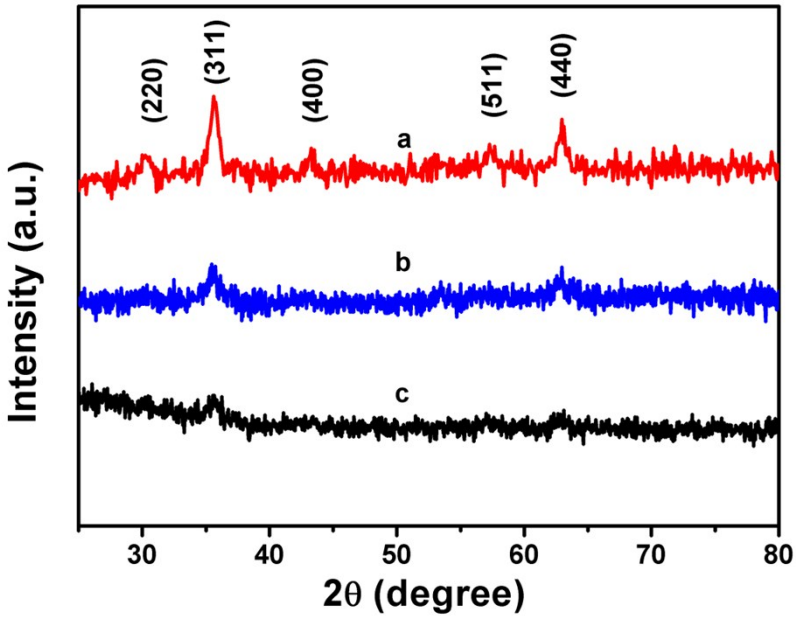

Fig. S1. XRD patterns of Fe_3O_4 (a), Fe_3O_4@β-CD (b) and reused Fe_3O_4@β-CD (c)

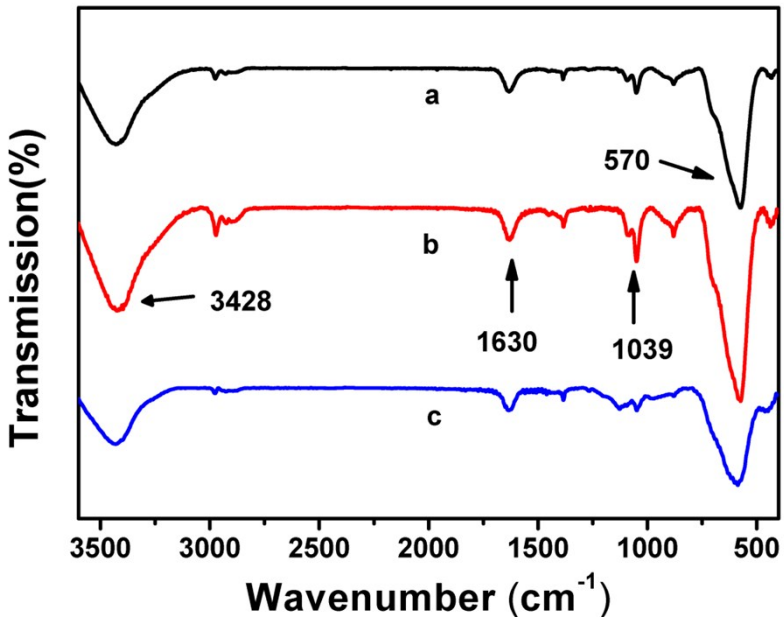

Fig. S2. FT-IR spectra of Fe_3O_4 (a), Fe_3O_4@β-CD (b) and reused Fe_3O_4@β-CD (c)

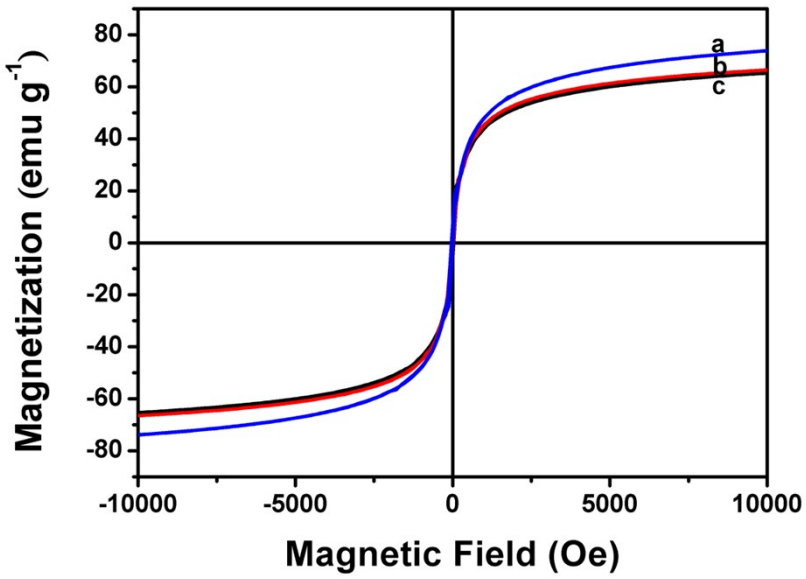

Fig. S3. Magnetization curves of Fe_3O_4 (a), Fe_3O_4@β-CD (b) and reused Fe_3O_4@β-CD (c)

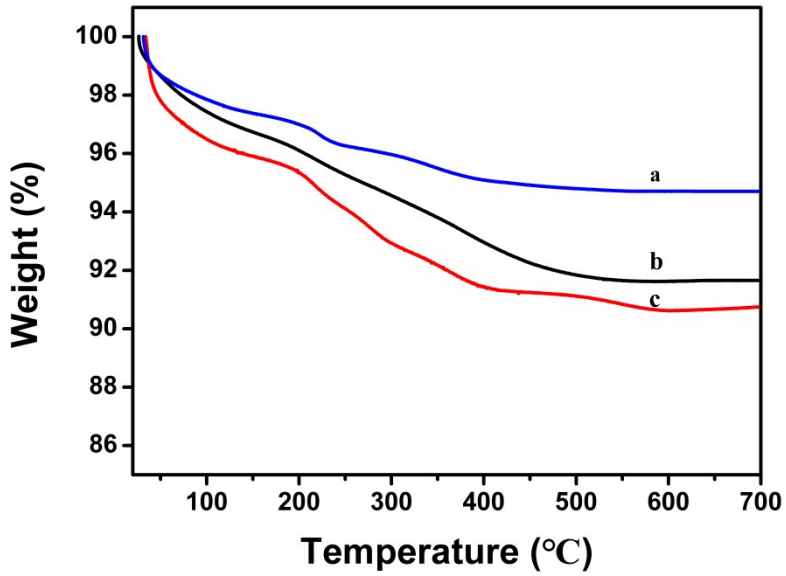

Fig. S4. TGA curves of Fe_3O_4 (a), Fe_3O_4@β-CD (b) and reused Fe_3O_4@β-CD (c)

Text S4:

The TGA curves of Fe_3O_4, Fe_3O_4@β-CD and reused Fe_3O_4@β-CD were displayed in Figure S4. The TGA curves presented the first weight loss before 200 °C and this could be explained by the removal of the adsorbed solvent (water and ethanol) attached to the catalysts surfaces. Then there was a distinction mass weight loss

between 200 and 550 °C, which may be caused by decomposition of Fe_3O_4 and β-CD. The weight loss of Fe_3O_4, Fe_3O_4@β-CD and reused Fe_3O_4@β-CD were 2.28%, 4.56% and 4.43% from 200 to 550 °C, respectively. Therefore, the amount of β-CD on the surface of Fe_3O_4 was 2.28% and Fe_3O_4@β-CD before and after use was determined as stable.

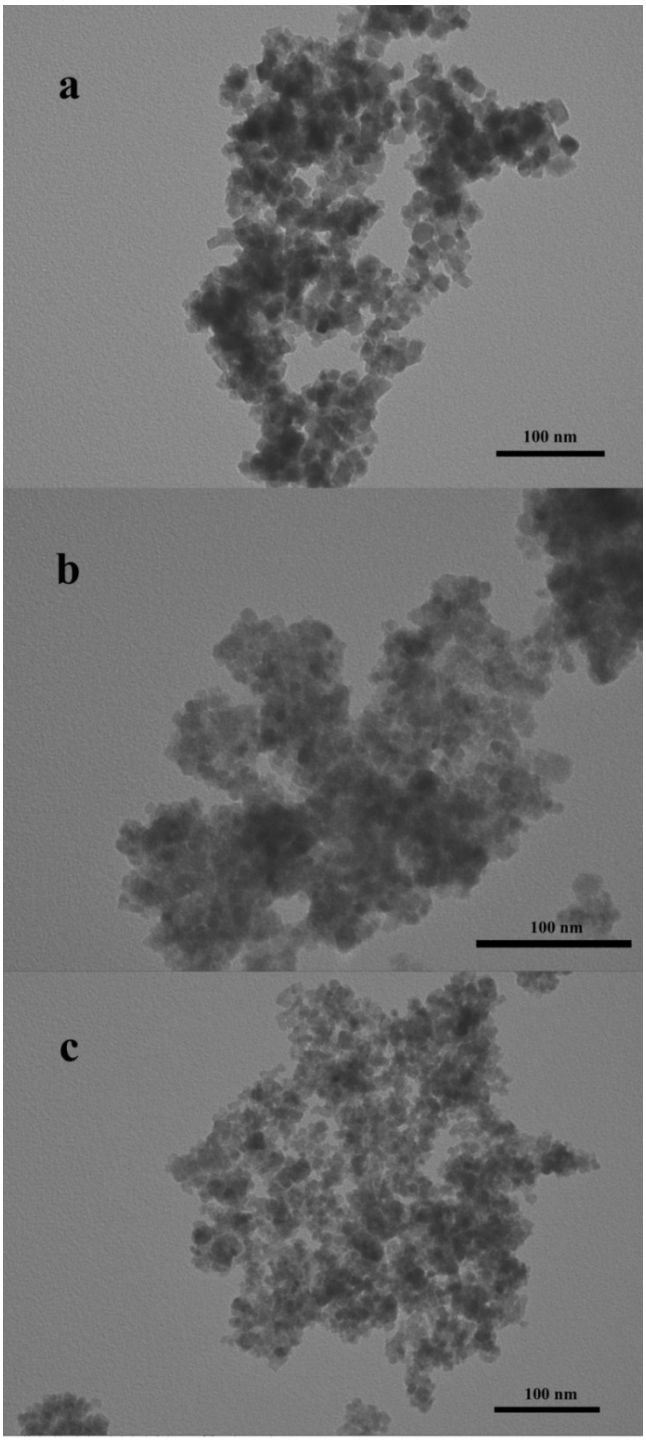

Fig. S5. TEM images of Fe_3O_4 (a), Fe_3O_4@β-CD (b) and reused Fe_3O_4@β-CD (c)

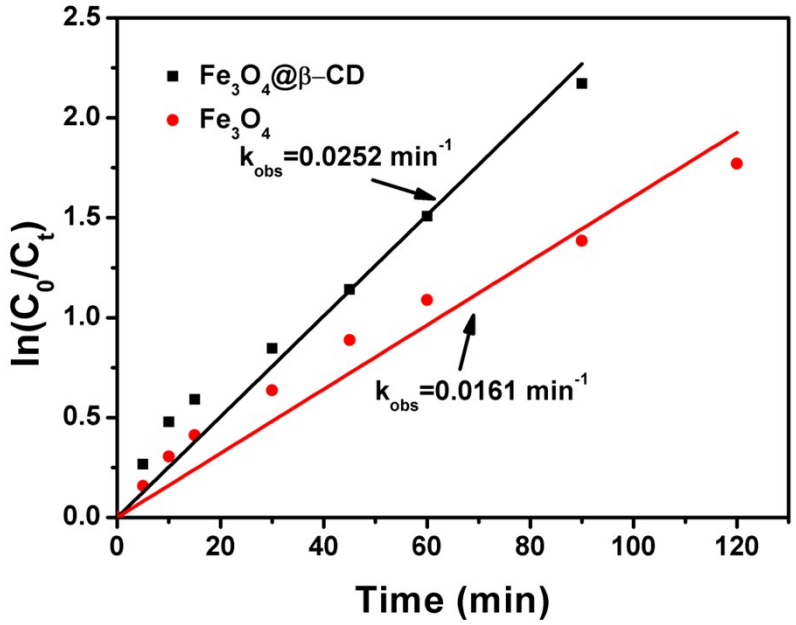

Fig. S6. Comparison of Fe_3O_4@β-CD and Fe_3O_4 for BPA degradation. Conditions: [BPA] = 0.1 mM, [PS] = 5 mM, [Fe_3O_4] = 1.0 g/L, [Fe_3O_4@β-CD] = 1.0 g/L, pH 3.0 and 25 °C.

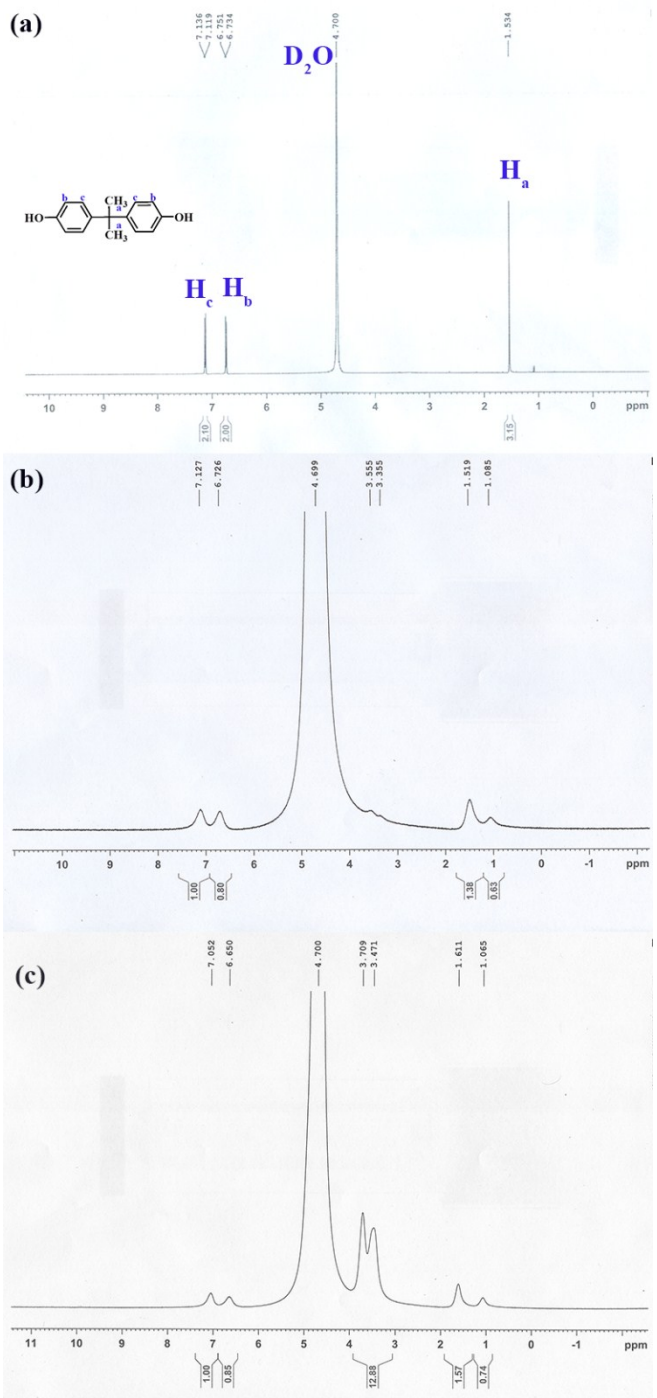

Fig. S7. The ^{1}H NMR spectra in D_2O of pure BPA (a), Fe_3O_4/BPA (b), and Fe_3O_4@β-CD/BPA (c).

Text S5:

Fig .S7 (a) showed two characteristic signal peaks of BPA (H_c and H_b), leading to two distinct resonances at 7.13 and 6.73 ppm. The signals at 1.53 ppm (H_a) belonged to CH_3-. A detailed investigation of ^{1}H NMR spectra of Fe_3O_4/BPA and Fe_3O_4@β-CD/BPA was operated to determine the formation of complex. As shown in Fig. S7

(b), the chemical shifts at 7.13, 6.73 and 1.52 of Fe_3O_4/BPA were the similar as pure BPA, indicating uncoated Fe_3O_4 could not form the complexes with BPA. However, the proton signals of Fe_3O_4@β-CD/BPA at 7.05, 6.65 and 1.61 ppm generated a minor shift in comparison to that of BPA and Fe_3O_4/BPA, suggesting the BPA molecule entering the β-CD cavity with H_a, H_b and H_c (Fig. S7 (c)). In brief, these minor chemical shift changes suggested that Fe_3O_4@β-CD from complexes with BPA.

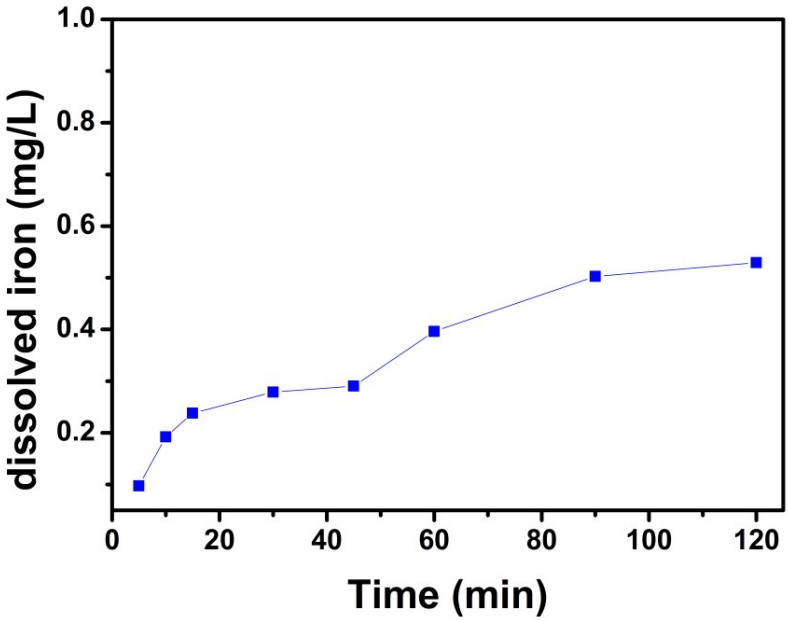

Fig. S8. Iron leaching during BPA degradation. Conditions: [BPA] = 0.1 mM, [PS] = 5 mM, [Fe_3O_4@β-CD] = 1.0 g/L, pH 3.0 and 25 °C.

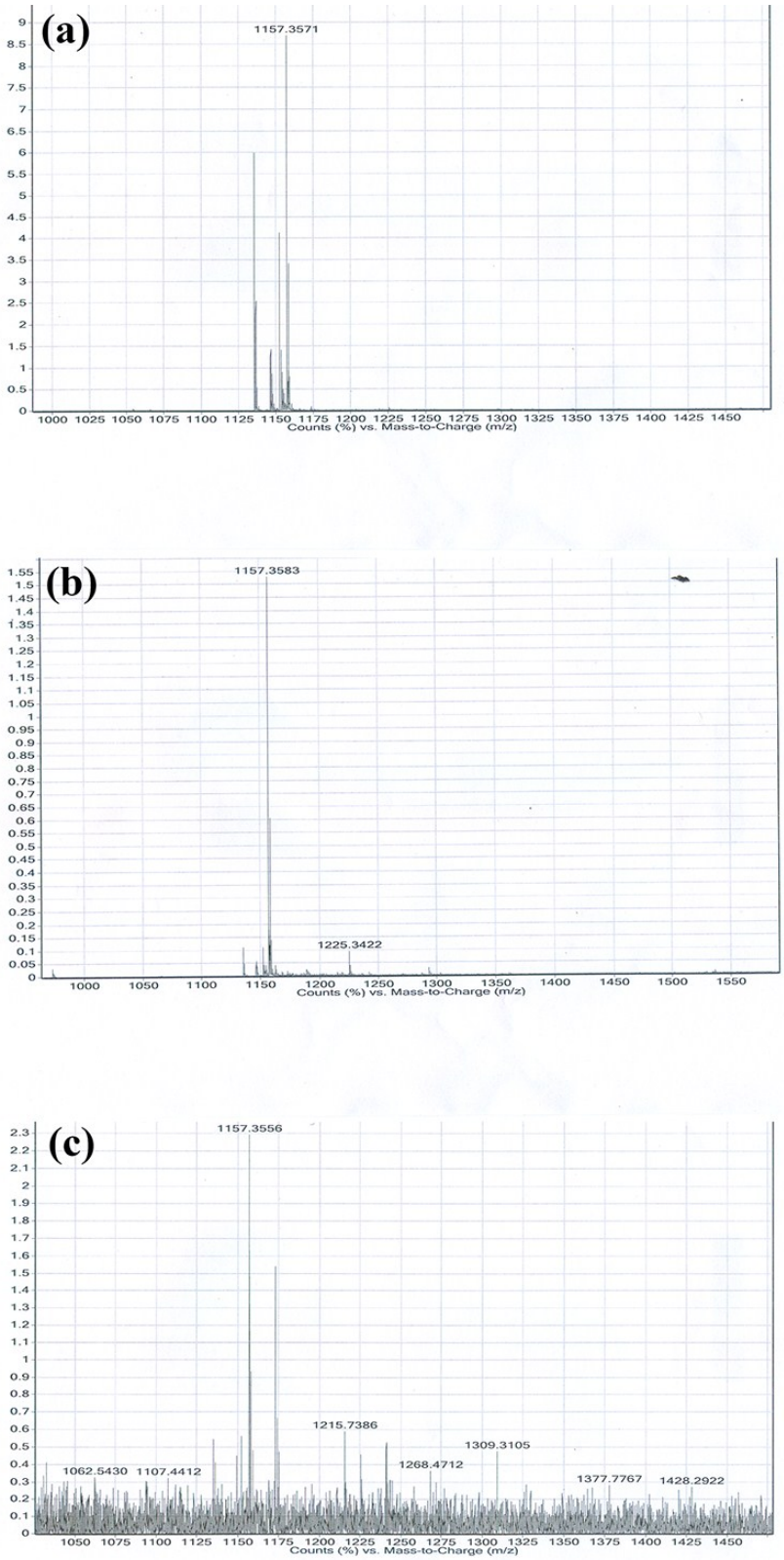

Fig. S9. Mass spectra of pure β-CD (a), Fe_3O_4@β-CD (b) and reused Fe_3O_4@β-CD (c)

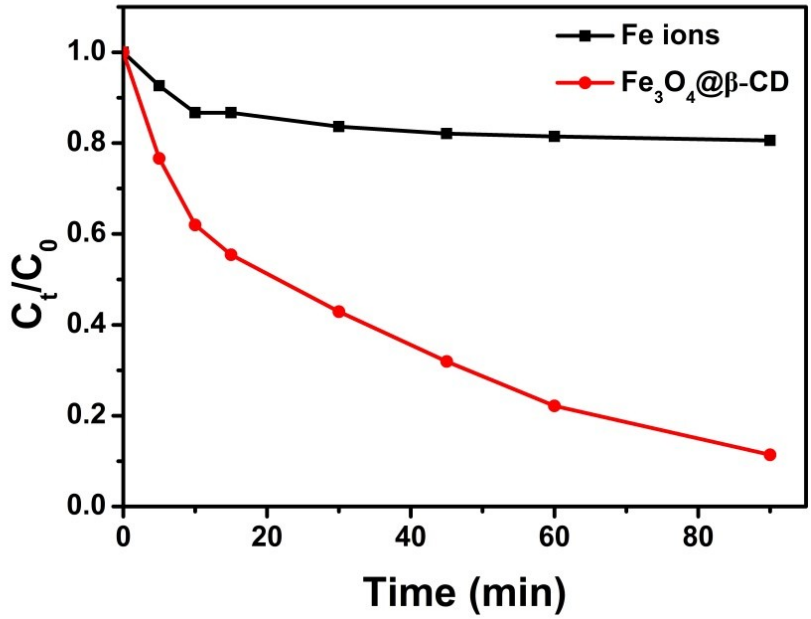

Fig. S10. The effect of homogeneous and heterogeneous catalysis on BPA degradation

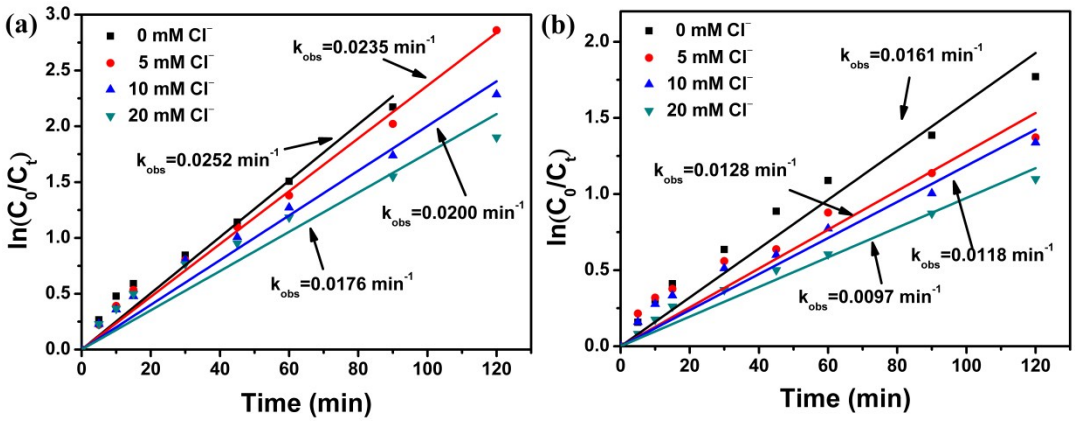

Fig. S11. Influence of Cl^- scavenger for BPA degradation in the Fe_3O_4@β-CD/PS system (a) and Fe_3O_4/PS system (b). Conditions: [BPA] = 0.1 mM, [PS] = 5 mM, [Fe_3O_4@β-CD] = 1.0 g/L, [Fe_3O_4] = 1.0 g/L, pH 3.0 and T = 25 °C.

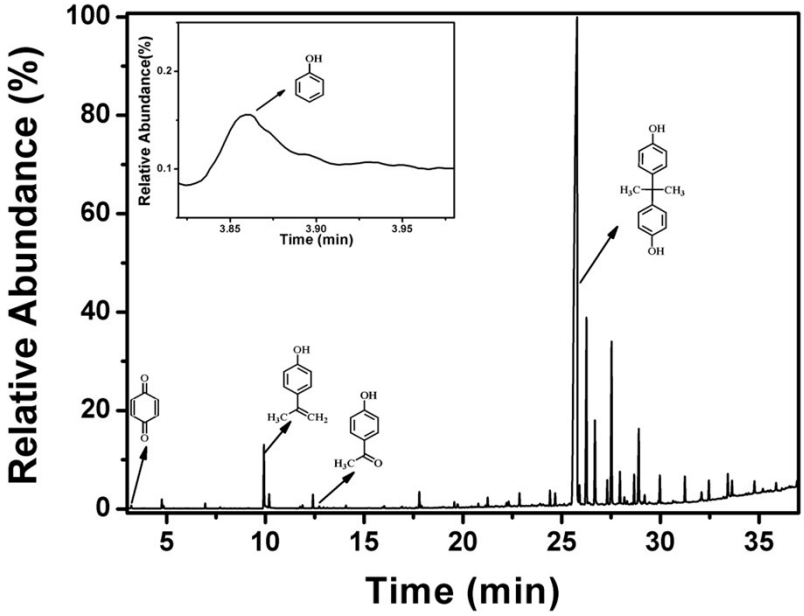

Fig. S12. GC diagram for BPA degradation after 60 min of reaction in the Fe_3O_4@β-CD/PS system.

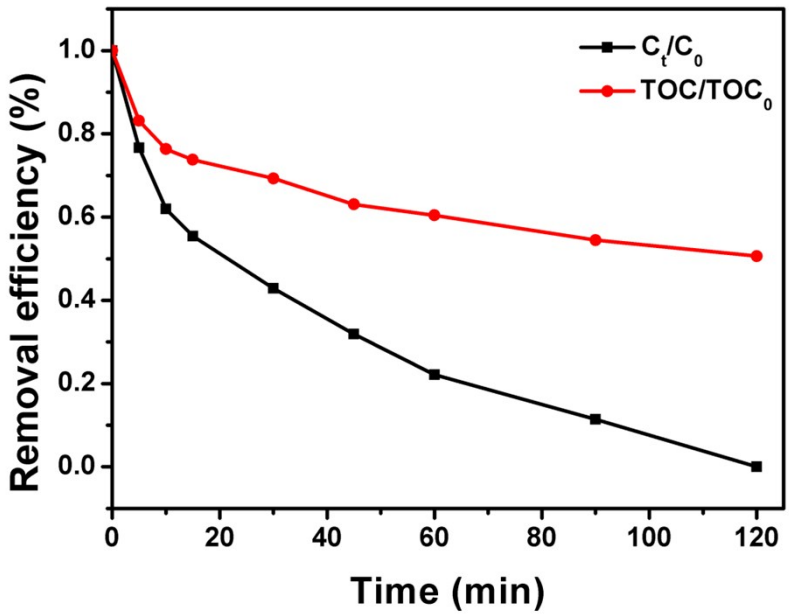

Fig. S13. Temporal change in BPA and TOC removal. Conditions: [BPA] = 0.1 mM, [PS] = 5 mM, [Fe_3O_4@β-CD] = 1.0 g/L, pH 3.0 and T = 25 °C.